ELSEVIER

Journal of Nuclear Materials 250 (1997) 244–249

journal of nuclear materials

Letter to the Editor

High resolution TEM of high burnup UO_2 fuel

K. Nogita *, K. Une

Nippon Nuclear Fuel Development Co., Ltd., 2163 Narita-cho, Oarai-machi, Higashi Ibaraki-gun, Ibaraki-ken 311-13, Japan

Received 3 April 1997; accepted 23 August 1997

Abstract

High-resolution TEM (HRTEM) observations and nano-area EDX analyses were carried out on small intragranular bubbles in the outer region of high burnup UO_2 pellets. Sample was prepered from the outer region of UO_2 pellet, which had been irradiated to the pellet average burnups of 49 GWd/t in a BWR. HRTEM observations and element analyses were made with a 200 KV cold-type field emission TEM (Hitachi FE-2000) having an ultra-thin window EDX (Noran Voyager). Lattice image and nano-area EDX results indicate the presence of 4-8 nm size Xe-Kr bubbles along with fission products of five metal particles, Mo-Tc-Ru-Rh-Pd. Nano-diffraction patterns from bubbles show two different new patterns besides matrix UO_2. From the Xe/U proportion obtained by nano-area EDX peak and nano-diffraction patterns from bubbles, it was concluded that Xe in the small bubbles was present in a solid or near solid state at very high pressure. Furthermore, from the results of high resolution images and diffractions obtained from recrystallized grains in rim structure region, neighboring recrystallized grains were clarified to be present with high angle grain boundaries. © 1997 Elsevier Science B.V.

1. Introduction

In the outer region of UO_2 pellets irradiated in light water reactors (LWRs), small intragranular bubbles of several nanometers in size are formed due to accumulation of fission-induced vacancies and the fission products Xe and Kr. The detailed characteristics of bubbles in UO_2 fuels irradiated to 1–83 GWd/t have been studied by transmission electron microscopy (TEM). The small bubbles of 1–3 nm in diameter observed in low burnup fuels (< 18 GWd/t) [1,2] appear to grow to 7–8 nm in high burnup fuel with 45–83 GWd/t [3–6]. Bubble density also increases with increasing burnup [4,5]. It has been thought that very high pressure fission gas atoms of Xe and Kr are present in these small bubbles [7]. Except for the Xe and Kr gas atoms, the fission product particles are found with to have a hcp structure (a solid-solution alloy of Mo–Tc–Ru–Rh–Pd) in the bubbles [8]. Thomas [8] estimated the density of Xe atoms in larger bubbles for irradiated UO_2 fuel pellets using TEM and energy dispersive X-ray spectroscopy (EDX). He showed that fission gas atoms of Xe were present at very high density in relatively larger bubbles of 50–80 nm, which were formed in the center to middle portion under high irradiation temperatures. Owing to the resolution limit of TEM/EDX analyses, density estimation of small intragranular bubbles, only a few nanometers in size, and also lattice images in irradiated UO_2 fuel pellet peripheries are still lacking. In our previous TEM studies of high burnup UO_2 fuel periphery [6], we found a recrystallized grain structure, as well as a high density of bubbles and dislocations. Thomas et al. [9] and we [5,6] proposed that these recrystallized grains have high angle grain boundaries with a random orientation based on results of selected area diffraction (SAD) patterns, though the exact angles between neighboring recrystallized grains are still not known.

In this paper, we observed and analyzed small intragranular bubbles, several nanometers in size, and dislocations, both in the defect cluster accumulation region and also recrystallized grains of the high burnup UO_2 fuel periphery. We used high resolution TEM (HRTEM) with nano-diffraction and nano-area EDX, which are powerful and innovative analytical techniques for high burnup UO_2 fuels.

* Corresponding author. Tel.: +81 29 2662131; fax: +81 29 2662589; e-mail: nogita@nfd.co.jp.

PII S0022-3115(97)00282-1

2. Experimental

The UO_2 fuel specimen examined in the present study was taken from the outer region of a UO_2 pellet (including the 'rim structure' formation region), which had been irradiated to the pellet average burnup of 49 GWd/t in a boiling water reactor (BWR). More detailed information on this specimen is available in Ref. [6].

The HRTEM sample was prepared by a crushing technique [10], which is widely used for preparation of HRTEM samples for ceramic and/or cleavage materials. The necessary thickness of the thin observation area to obtain the bubble densities and nano-EDX spectrum from small intragranular bubbles was determined by a thickness fringe [11]. HRTEM observations were made with a 200 kV cold-type field emission TEM (Hitachi FE-2000) equipped with an ultra-thin window EDX (Noran Voyager). The magnification of lattice images was $\times 1\,500\,000$ on the fluorescent screen. The areas of nano-diffraction and nano-EDX were about 3–5 and 2–3 nm in diameter, respectively. Some lattice images were treated using Fourier and inverse Fourier transformation image systems (Gatan Digital Micrograph™ image systems) to get clearer visible images of lattice defects.

3. Results and discussion

3.1. Lattice images and density estimation of small intragranular bubbles

Fig. 1 shows a lattice image and diffraction pattern of an irradiated UO_2 fuel pellet. The image was taken from interference of systematic $\langle 111 \rangle$ spots and the transmitted (center) spot. The stripes of this image correspond to UO_2 (111) planes, so that their spacing is about 3.16 Å. In this figure, there are many round shapes a few nanometers in size. These are assigned to fission gas bubbles. Their average diameter and number density are 4.4 nm and 4.3×10^{23} m^{-3}, respectively. These values are in good agreement with the results for the same specimen prepared by ion milling for examination [6]. The round shaped images have a different lattice image from the matrix UO_2 or Moiré fringe. This indicates the presence of a solid crystal structure with a different orientation and/or lattice parameter from the matrix UO_2 fluorite structure in the round shapes. Possible explanations of this extra lattice image (or Moiré fringe) are its being from (i) a solid Xe lattice, or (ii) five-metal (Mo–Tc–Ru–Rh–Pd) precipitates, though it is very difficult to distinguish between them only from these images.

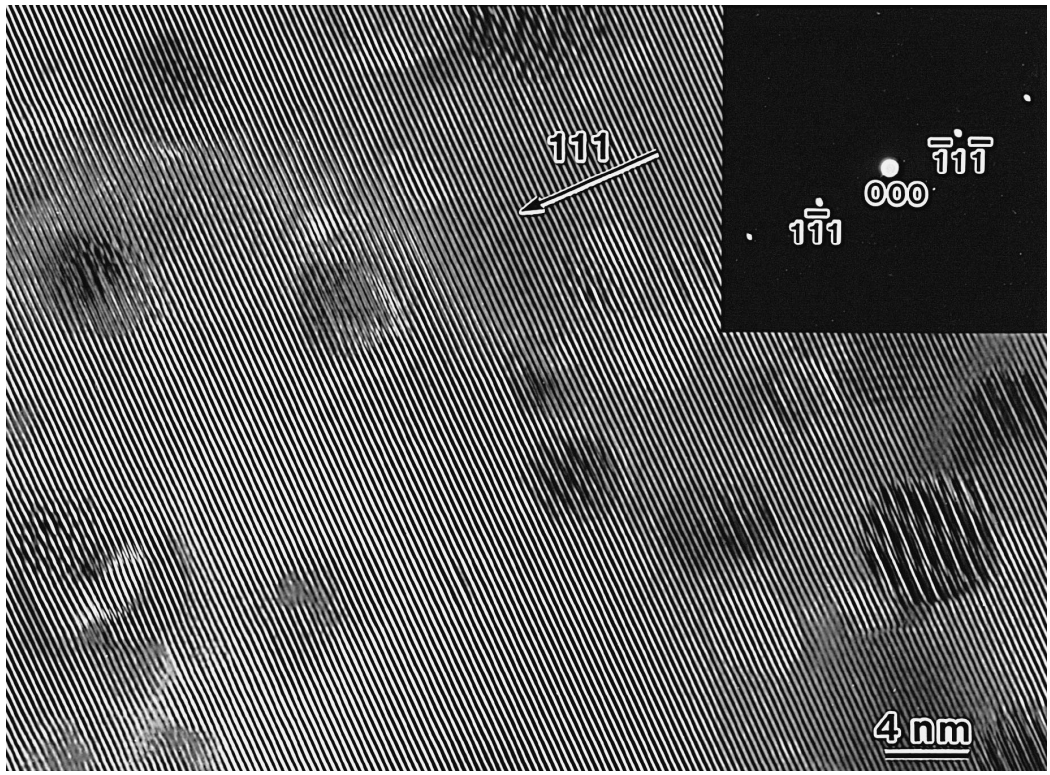

Fig. 1. Lattice image and diffraction pattern of irradiated UO_2 fuel. On the basis of observations described later in the text, we judged that there were FP gas atoms present with FP particles of five-metal precipitates.

Fig. 2 shows another lattice image, which was taken from the [110] crystal orientation. The nano-diffraction patterns of (A)–(C) were taken from the correspondingly lettered bubbles in Fig. 2. The diffraction patterns of (A) indicate a perfect UO_2 fluorite structure from the [110] direction. In addition to the matrix UO_2 diffraction spots, there are extra spots in (B) and (C). This indicates the existence of other solid particles in addition to the matrix UO_2 in these bubbles. From these results, we still can not say whether these extra spots are from solid Xe particles, because it is difficult to separate or distinguish them from spots of the five-metal precipitate. The five-metal precipitate is reported to have a hcp structure [8], though it is impossible to determine any structure from just these extra spots in (B) and (C) so far. We are continuing to work on the problem and will report in another paper sometime. We note that (C) in Fig. 2 shows two different kinds of spots in addition to the spots from matrix UO_2. They may indicate the presence of solid Xe particles and five-metal precipitates in the same bubble. Presence of solid inert gas is not a new phenomenon. Hashimoto et al. [12] and Yagi et al. [13] found solid Kr particles in 50 keV Kr-implanted Al metal. Selected area electron diffraction patterns exhibited extra reflection spots, indicating the presence of solid Kr precipitates which had grown epitaxially with the host Al crystal. In the case of our results in Fig. 2, nano-diffraction spots indicate (either solid Xe or five-metal precipitate) the random growth of solid particles instead of epitaxial growth with the matrix UO_2.

The nano-EDX spectrum from bubbles indicates Xe presence in the bubbles. Following the simple modification of the Cliff–Lorimer ratio analysis of thin foils which was applied by Thomas [8] for bubbles in irradiated UO_2 fuels, the density of Xe particles can be obtained by Eq. (1) using EDX peak intensities and thickness

$$\left(\rho_{\mathrm{Xe}}/\rho_{\mathrm{UO_2}}\right) = \left(k_{\mathrm{Xe-U}}\right)\cdot\left(I_{\mathrm{Xe}}/I_{\mathrm{U}}\right)\cdot\left(t_{\mathrm{UO_2}}/t_{\mathrm{Xe}}\right), \qquad (1)$$

where ρ is the density, $k_{\mathrm{Xe-U}}$ is the calculated k-factor (for $\mathrm{Xe}_{\mathrm{L}\alpha}$ and $\mathrm{U}_{\mathrm{L}\alpha}$, $k_{\mathrm{Xe-U}} = 0.524$), I is X-ray peak intensity, and t is the thickness. Density results from three bubbles determined with an estimated accuracy of $\pm 50\%$

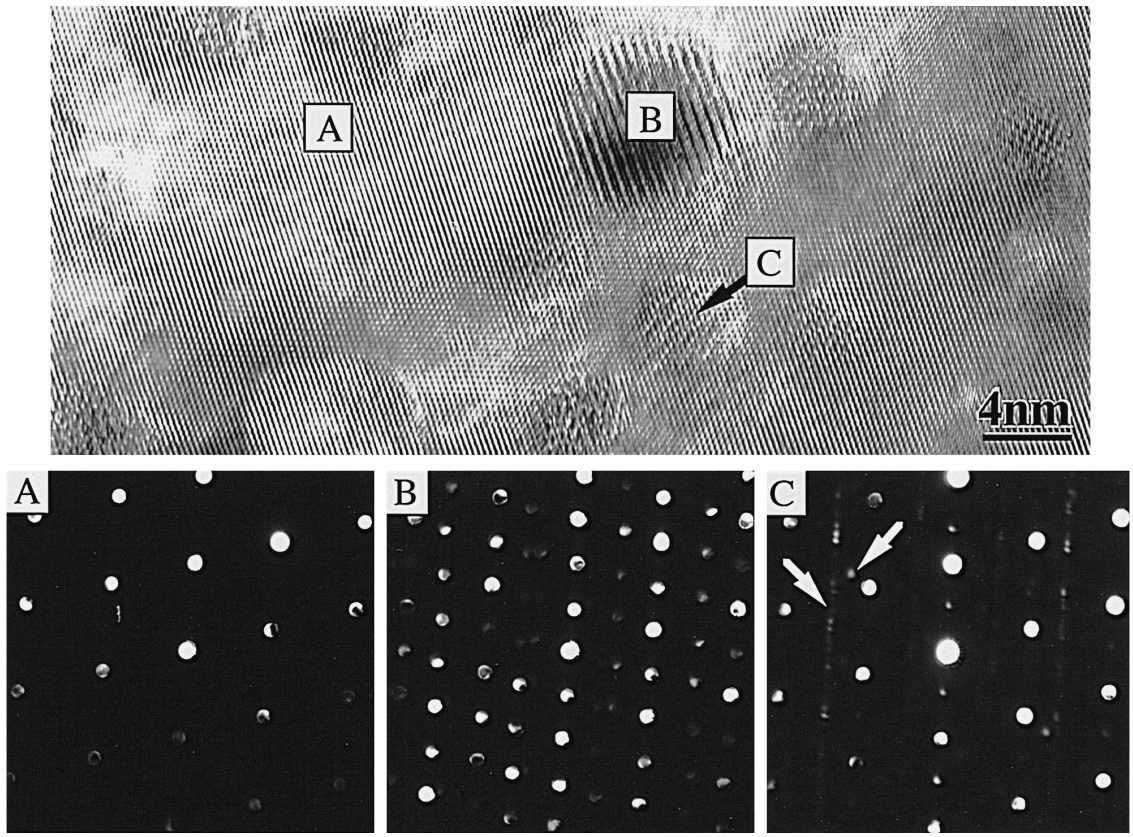

Fig. 2. Lattice image of irradiated UO_2 fuel obtained from the [110] direction and nano- diffraction patterns from correspondingly lettered areas in the image. (A) shows a diffraction pattern from the matrix UO_2. (C) shows two different kinds of spots in addition to the spots from the matrix UO_2.

Table 1
Density estimation of Xe bubbles

Bubble diameter (nm)	I_{Xe}/I_U	t_{UO_2}/t_{Xe}	Density (g/cm^3)
4.0	0.5	1.0	5.3
5.0	0.4	2.0	4.0
8.0	0.5	1.3	6.0

[8] are given in Table 1. The bubbles with 4–8 nm in size observed by nano-EDX have roughly Xe densities of 4–6 g/cm^3. We cannot determine the structure of solid Xe in the bubbles, though if solid Xe is precipitated in a face-centered cubic structure with a lattice parameter of 6 Å, its density is expected to be about 4 g/cm^3, so that our EDX result may suggest the presence of solid Xe. In addition to the Xe, the nano-EDX spectrum also shows X-ray peaks for a five-metal precipitate in the bubble with an approximate composition of 44 wt% Mo, 13 wt% Tc, 20 wt% Ru, 12 wt% Rh and 11 wt% Pd, roughly in proportion to the fission yields. This result indicates that even in small bubbles, only nanometers in size, five-metal precipitates exist in proportion to the fission yields with Xe atoms.

From the lattice images and nano-diffraction patterns, with the lattice showing Xe peaks in small bubbles of several nanometer size, we conclude that Xe atoms in the bubbles are present at very high density. The next study will need to make more detailed and thorough quantitative estimations, e.g., matrix thickness estimation and Xe peak intensity, and to establish a relationship between lattice image and nano-diffraction.

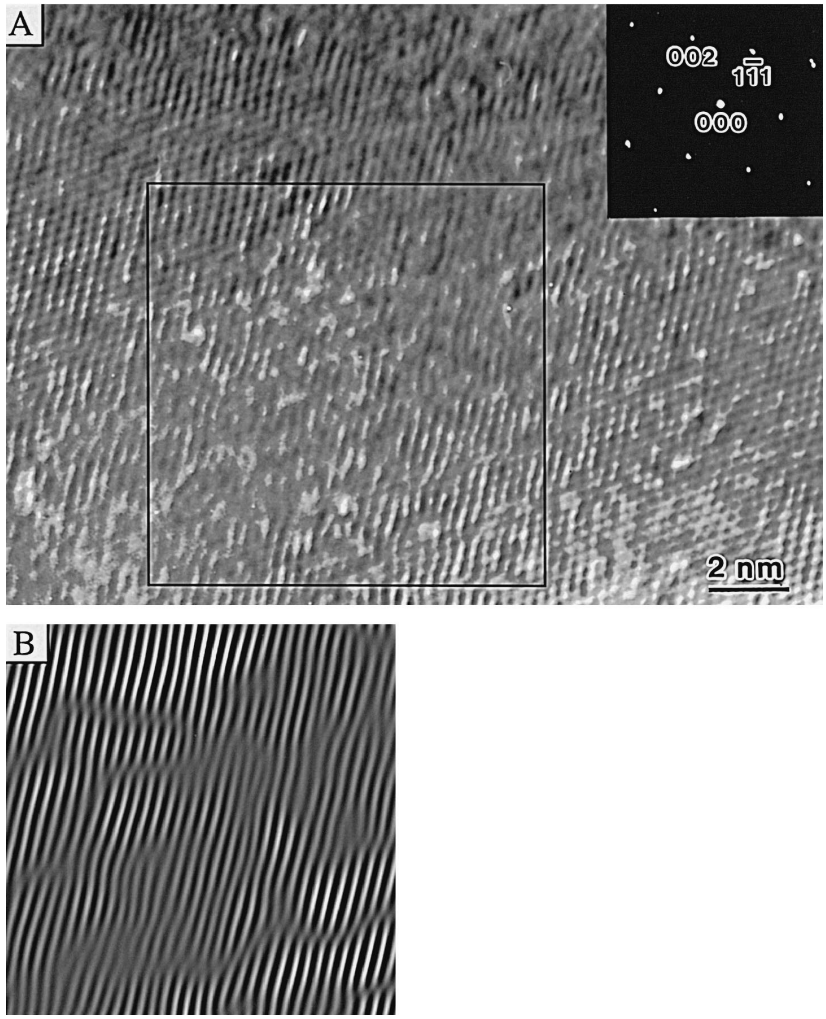

Fig. 3. (A) Lattice image of a dislocation accumulation region from the [110] orientation; (B) the filtered image taken from the framed area in A showing a high density of dislocations.

3.2. Angle measurement of neighboring recrystallized grains in rim structure formation region

We proposed a formation mechanism for rim structure [5,6] in the high burnup fuel pellet periphery, which is directly related to the accumulation of fission damage. Tangled dislocation networks with low angle grain boundaries are formed by the inhomogeneous accumulation of dislocations after the development of interstitial-type dislocation loops. Tangled dislocations are organized into subdivided grains with high angle boundaries. Then, some of them are recrystallized, sweeping out small intragranular bubbles. Therefore, in the rim structure region (this TEM sample), the following three different areas are inhomogeneously distributed: (i) an irradiation-induced defect cluster (bubbles and dislocations) accumulation area, (ii) a few nanometer size grain (nucleus grains of recrystallization) accumulation area, and (iii) a recrystallized grain formation area with 100–300 nm grains. In Fig. 3, we observe low angle grain boundaries with few nanometer-sized grains in area (ii). Fig. 3(A) shows a lattice image from the [110] orientation. With an inverse Fourier transform using the two ⟨111⟩ spots, a filtered image is obtained in Fig. 3(B) showing the matrix (111) plane clearly. This image of the (111) plane demonstrates that the crystal has been divided with slightly different orientations by a high density of dislocations. This image is expected to correspond to the 'embryo' or origin of nucleus for recrystallization. A similar dislocation image was obtained by Matzke and Wang [14] in Xe-ion (0.5 MeV) irradiated UO_2.

From low magnification bright-field images of the recrystallized region, we obtain an average grain size of recrystallized grains of about 80 nm. This size is relatively smaller than our previously reported data (170 nm) [6], due to different TEM sample preparations. Thomas et al. [9] and we [5,6] proposed that these recrystallized grains have high angle grain boundaries with random orientation on the basis of results of SAD patterns. We tried to observe the region of newly formed grain boundaries of recrystallized grains by lattice images and we got the angle between neighboring recrystallized grains by nano-diffraction analysis. Fig. 4 shows a lattice image and nano-diffraction patterns of the recrystallized regions including grain boundaries. First of all, the (A) area in Fig. 4 was taken from systematic ⟨111⟩ spots and the center spot. This means that stripes of the lattice image in (A) correspond to the (111) plane or are perpendicular to the ⟨111⟩ direction. Then, the nano-diffraction pattern was taken from the (B) area without any angle modifications. The angle between the (111) plane from the (B) grain and that from the (A) grain is the angle of these two grains and is 43°.

From the results of high resolution images and diffrac-

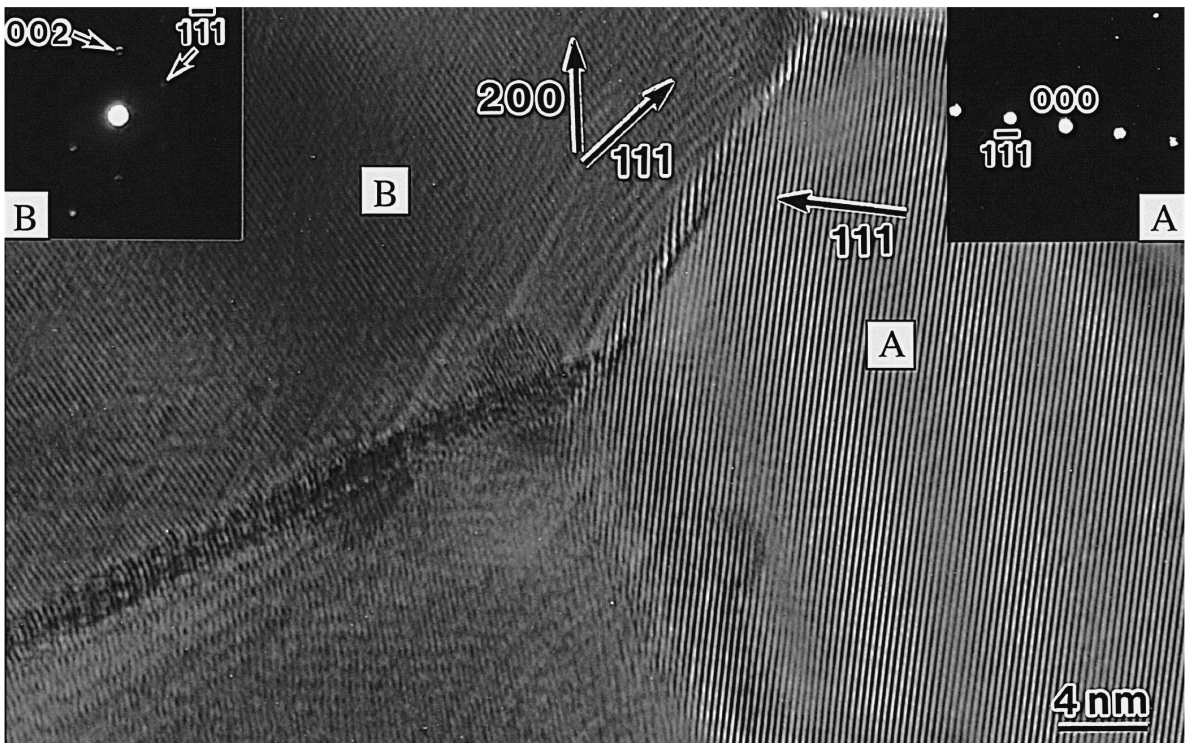

Fig. 4. Lattice image and nano-diffraction patterns from the recrystallized region. Nano-diffraction patterns of (A) and (B) are taken from the positions (A) and (B) in the lattice image. The angle between (A) and (B) grains is 43° for the (111) plane.

tion patterns obtained from recrystallized grains in the rim structure region, we conclude that neighboring recrystallized grains are present with high angle grain boundaries.

Acknowledgements

We would like to thank Professor C. Kinoshita and Associate Professor S. Matsumura of Kyushu University (Department of Nuclear Engineering and Laboratory of High Voltage Electron Microscopy) for valuable discussions on HRTEM images and nano-area electron diffraction/EDX analyses.

References

[1] R.M. Cornell, J. Nucl. Mater. 38 (1971) 319.
[2] C. Baker, Eur. App. Res. Rept.-Nucl. Sci. Technol. 1 (1979) 19.
[3] I.L.F. Ray, H. Thiele and Hj. Matzke, in: S.E. Donnelly, J.H. Evans (Eds.), Fundamental Aspects of Inert Gases in Solids, Plenum, New York, 1991, p. 457.
[4] S. Kashibe, K. Une, K. Nogita, J. Nucl. Mater. 206 (1993) 22.
[5] K. Nogita, K. Une, Nucl. Instrum. Meth. B91 (1994) 301.
[6] K. Nogita, K. Une, J. Nucl. Mater. 226 (1995) 302.
[7] Hj. Matzke, in: S.E. Donnelly, J.H. Evans (Eds.), Fundamental Aspects of Inert Gases in Solids, Plenum, New York, 1991, p. 401.
[8] L.E. Thomas, in: S.E. Donnelly, J.H. Evans (Eds.), Fundamental Aspects of Inert Gases in Solids, Plenum, New York, 1991, p. 431.
[9] L.E. Thomas, C.E. Beyer, L.A. Charlot, J. Nucl. Mater. 188 (1992) 80.
[10] K. Nogita, K. Une, J. Nucl. Sci. Technol. 30 (9) (1993) 900.
[11] P.B. Hirsch, A. Howie, R.B. Nicholson, D.W. Pashley, M.J. Whelan, Electron Microscopy of Thin Crystals, Butterworth, London, 1965.
[12] I. Hashimoto, H. Yorikawa, H. Mitsuya, H. Yamaguchi, K. Takaishi, T. Kikuchi, K. Furuya, E. Yagi, M. Iwaki, J. Nucl. Mater. 149 (1987) 69.
[13] E. Yagi, I. Hashimoto, H. Yamaguchi, J. Nucl. Mater. 169 (1989) 158.
[14] Hj. Matzke, L.M. Wang, J. Nucl. Mater. 231 (1996) 155.